ELSEVIER

Palaeogeography, Palaeoclimatology, Palaeoecology 187 (2002) 83–100

PALAEO

www.elsevier.com/locate/palaeo

Carbon isotope ($\delta^{13}C$) stratigraphy across the Silurian–Devonian transition in North America: evidence for a perturbation of the global carbon cycle

Matthew R. Saltzman *

Department of Geological Sciences, Ohio State University, Columbus, OH 43210, USA

Received 16 October 2001; received in revised form 4 June 2002; accepted 18 July 2002

Abstract

Carbon isotope ($\delta^{13}C$) analyses of marine carbonates spanning the Silurian–Devonian transition are compared from three richly fossiliferous, well-dated sequences in North America. The three sections, in the central Appalachian Mountains (West Virginia), Great Basin (Nevada), and the southern Mid-continent (Oklahoma), reveal positive $\delta^{13}C$ shifts beginning in the late Pridoli and reaching peak values as heavy as +5.8‰ in the earliest Lochkovian following the first occurrence of the conodont species *Icriodus woschmidti* and the graptolite *Monograptus uniformis*. A positive shift in $\delta^{13}C$ is also recorded at this time in Gondwanan regions, including the global stratotype section and point for the Silurian–Devonian boundary at Klonk in the Czech Republic, as well as in sections in the Carnic Alps of Austria (Cellon), and Queensland, Australia. The available data from Euramerica and Gondwana are consistent with a scenario linking seawater $\delta^{13}C$ enrichment to a eustatic drop during the Silurian–Devonian transition. Seawater $\delta^{13}C$ likely increased as a result of enhanced carbonate weathering during exposure and erosion of older Silurian platform deposits. In addition, the fall in sea level appears to have enhanced nutrient delivery to the oceans and triggered an increase in organic carbon burial rates at or near the Silurian–Devonian boundary, as indicated by organic-rich deposition in Gondwanan basins. In terms of its magnitude, the Silurian–Devonian $\delta^{13}C$ excursion of $\geq$+5‰ appears to be among the largest well-documented events in the Paleozoic, comparable to the shifts in the Late Ordovician and Early Mississippian.

Keywords: Silurian–Devonian boundary; carbon isotope; sea level; conodont; graptolite

1. Introduction

The Silurian–Devonian boundary was the first systemic boundary to be subject to intensive worldwide scrutiny using modern stratigraphic methods and procedures (Chlupac and Kukal, 1977a,b; Cowie et al., 1986; Chlupac and Hladil, 2000). Beginning with the First International Symposium held in Prague, Czechoslovakia in 1958 and culminating with the final meeting of the International Union of Geological Sciences Silurian–Devonian Boundary Committee in Montreal in 1972, the search for the stratotype has provided an extensive literature for all regions of

* *E-mail address:* saltzman.11@osu.edu (M.R. Saltzman).

0031-0182/02/$ – see front matter
PII: S0031-0182(02)00510-2

significant outcrop area and important fossil groups worldwide (e.g. Berdan et al., 1969; Flugel et al., 1977). Following the selection of the base of the *Monograptus uniformis* graptolite zone at Klonk in the Prague Basin of the Czech Republic as the global stratotype section and point (GSSP), numerous studies have continued to refine the biostratigraphic and sedimentologic context of the Silurian–Devonian (Pridolian–Lochkovian) boundary in successions both within the stratotype area and in different biogeographic realms (Berry and Murphy, 1975; Klapper and Murphy, 1975; Denkler and Harris, 1988; Jeppsson, 1989; Hladil, 1991). This work has provided the essential framework for more recent investigations aimed at characterizing the chemical stratigraphy (i.e. stable isotopic and trace elemental) of the Silurian–Devonian transition as a means of reconstructing dynamics of ocean circulation, climate and carbon cycling (Schonlaub et al., 1994; Hladikova et al., 1997; Porebska and Sawlowicz, 1997; Buggisch, 2001). However, to this point, detailed geochemical studies have been conducted only for Gondwanan basins and not the Euramerican realm that lay opposite the Rheic Ocean (Fig. 1; Witzke, 1990; Scotese and McKerrow, 1990), and thus the global significance of observed trends is uncertain.

The purpose of this paper is to present high-resolution carbon isotope ($\delta^{13}C$) data from widely separated basins of the ancient Euramerican land mass that can be used to evaluate the significance of stable isotopic ($\delta^{13}C$) trends from the Silurian–Devonian transition at the GSSP in the Prague Basin and other regions of Gondwana (Fig. 1). The $\delta^{13}C$ trends identified at Klonk by Hladikova et al. (1997) and Buggisch (2001), along with the section at Cellon in the Carnic Alps (Schonlaub et al., 1994), show a substantial positive shift of $\sim$+4‰ across the Silurian–Devonian boundary which the authors relate to enhanced surface–ocean productivity and high rates of organic matter burial. Further insight into the processes that generated this positive $\delta^{13}C$ excursion, which is similar in magnitude to several events recently documented from lower down in the Silurian

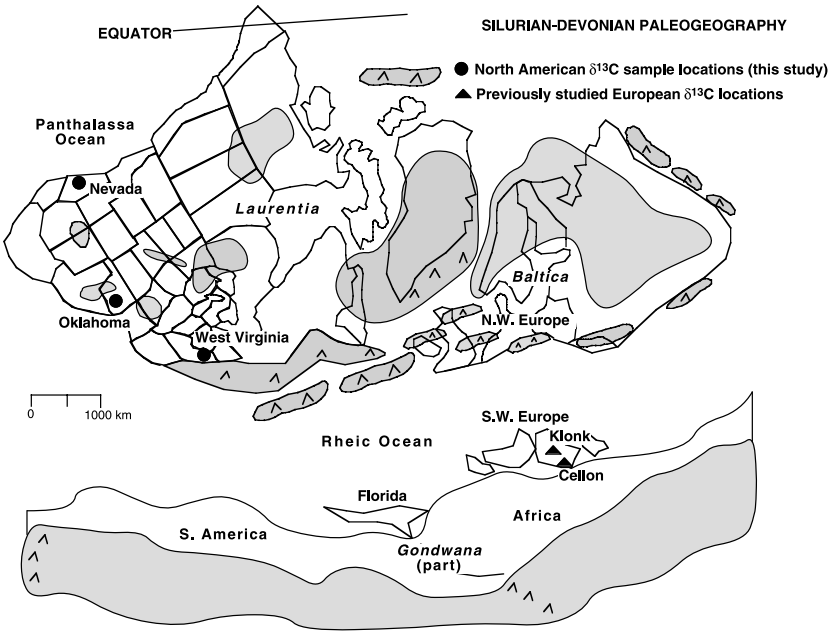

Fig. 1. Locality map (after Witzke, 1990; including part of Gondwana after Scotese and McKerrow, 1990) showing positions of sections in central Nevada, eastern West Virginia, and southern Oklahoma sampled for $\delta^{13}C$, along with previously studied localities in Europe (Czech Republic and Austria) discussed in text. Shading is land, triangle pattern mountains.

(Azmy et al., 1998; Saltzman, 2001), can come only with a more complete knowledge of the $\delta^{13}C$ record worldwide and its relationship to organic-rich deposition, shifting facies patterns and changes in sea level. Three North American successions presently stand out as particularly suitable for comparison with the $\delta^{13}C$ trends observed in Gondwana because they occur in carbonate depositional regimes and contain either conodont or graptolite species that mark the position of the boundary within a relatively narrow stratigraphic interval, including: (1) the Roberts Mountains Formation in the Roberts Mountains of central Nevada (Berry and Murphy, 1975; Klapper and Murphy, 1975); (2) the Helderberg Group in the central Appalachian Mountains of eastern West Virginia (Denkler and Harris, 1988); and (3) the Hunton Group in the Arbuckle Mountains of south-central Oklahoma (Barrick and Klapper, 1992). These results from integrated biostratigraphic, sedimentologic and chemostratigraphic studies of the Silurian–Devonian transition offer a unique opportunity to reconstruct Earth history for a single, well-defined time slice, and represent an ideal framework within which to observe the global scope and significance of the $\delta^{13}C$ record.

2. Regional setting

The Silurian–Devonian transition is known to be preserved in a limited number of localities in North America that represent either rapidly subsiding portions of foreland basins (central Appalachians; Dorobek and Read, 1986; Denkler and Harris, 1988) and aulacogens (Arbuckle region; Barrick and Klapper, 1992; Johnson, 1993), or relatively deep-water outer shelf to slope environments (Great Basin region; Matti and McKee, 1977; Poole et al., 1977; Sheehan and Boucot, 1991). This spotty record of continuous sedimentation reflects a period of extensive pre-Middle Devonian erosion associated with the drop in sea level that formed Tippecanoe–Kaskaskia megasequence boundary of Sloss (1963), ultimately removing much of the latest Silurian and early Devonian from Nevada to New York (Dennison and Head, 1975; Johnson and Murphy, 1984; Witzke and Bunker, 1996).

2.1. Appalachian Basin

In the Appalachian Mountain region, the Silurian–Devonian transition (late Pridolian and early Lochkovian) is best developed near the axis of the Appalachian Foreland Basin in the Valley and Ridge Province of the Virginia–West Virginia–Maryland region where it occurs within the Helderberg Group (Denkler and Harris, 1988). The Helderberg Group is a heterogeneous succession of open-marine, mixed carbonate and siliciclastic facies that formed during a period of relative tectonic quiescence between the major developments of the Taconic and Acadian clastic wedges (Dorobek and Read, 1986). To the north of the axis of the Helderberg Basin in New York and New Jersey, the precise location of the Silurian–Devonian transition is less well known due a thinner, more restricted succession that includes evaporite deposits, and quartzose and mud-cracked dolomites of the Rondout Formation and associated units (Head, 1969; Denkler and Harris, 1988). Other areas of the Appalachian region in which the Silurian–Devonian boundary interval has not been removed by pre-Middle Devonian erosion (Wallbridge Discontinuity of Dennison and Head, 1975) include more clastic-rich sections to the north on the Gaspé Peninsula of Quebec (Gascons and West Point formations; Borque and Lesperance, 1977), and the Arisaig area of Nova Scotia and eastern Maine (Stonehouse Formation; Berdan et al., 1969).

2.2. Great Basin and Rocky Mountains region

In the western United States, the Silurian–Devonian boundary interval is known within a relatively narrow, north–south oriented strip of richly fossiliferous, outer shelf sediments in central Nevada included within the Roberts Mountains Formation and equivalents (Berry and Murphy, 1975; Matti and McKee, 1977). To the east (landward) of this favorable depositional setting in central Nevada, large areas of eastern Nevada and Utah are dominated by unfossiliferous to sparsely

fossiliferous dolomite (Lone Mountain Dolomite) and restricted peritidal to supratidal facies (Laketown Dolomite) that obscure the identification of the boundary interval and may represent a major sedimentary hiatus spanning much of the Pridolian and lower Lochkovian (Johnson and Murphy, 1984; Sheehan and Boucot, 1991). In the present day Northern Rocky Mountain region, vast areas of Wyoming, northern Arizona, eastern Utah and Colorado have been stripped of Silurian rocks entirely, displaying a major unconformity with Middle to Upper Devonian strata in stratigraphic contact with underlying Cambrian or Ordovician units (Poole et al., 1977; Sheehan and Boucot, 1991).

2.3. USA mid-continent

The Silurian–Devonian transition in the USA mid-continent is well developed in the southern Oklahoma region of the Arbuckle Mountains where a relatively thick (~40 m) sequence of predominantly fine-grained, argillaceous limestones was deposited within the Oklahoma aulacogen to form parts of the Henryhouse and Haragan formations of the Hunton Group (Amsden, 1962, 1988; Barrick and Klapper, 1992; Johnson, 1993). Elsewhere, in the more northerly parts of the mid-continent region, the Upper Silurian succession is dominated by restricted carbonate facies that remain poorly dated. For example, in central Iowa, tens of meters of laminated and mounded dolomites (Gower Formation) can only be confidently assigned an age no younger than Wenlockian (Witzke and Bunker, 1996). Similarly restricted and sparsely fossiliferous reef facies, indicative of hypersaline environments, are developed in the upper Silurian of the Michigan Basin and adjacent regions of Wisconsin, Illinois and Indiana (Shaver, 1996). Only to the south of this dolomitic, reef-dominated facies belt is another reasonably well-dated transition from the Silurian to the Devonian recorded within a patch of fine-grained, shelf-edge limestones and graptolitic shales in southeastern Missouri (Bainbridge facies; Berry and Satterfield, 1972).

The three North American successions targeted for stable isotopic investigation are complementary in that the central Nevada succession represents one of the thickest Siluro–Devonian sequences worldwide in which both conodont and graptolite faunas have been described (Berry and Murphy, 1975; Klapper and Murphy, 1975); south-central Oklahoma contains one of the most densely sampled and integrated conodont and macrofossil successions in North America (Amsden, 1962, 1988; Barrick and Klapper, 1976, 1992); and sections in West Virginia are the best documented from a perspective of sequence stratigraphy and basin analysis (Head, 1969; Dorobek and Read, 1986). Taken together, the biostratigraphic and lithostratigraphic frameworks in place in the three regions afford a relatively high level of confidence in making direct comparisons of $\delta^{13}C$ trends and sea-level curves derived from Euramerica with the previously examined GSSP succession at Klonk in the Prague Basin and other Gondwanan regions (Fig. 1).

3. Methods

In order to generate high-resolution curves, $\delta^{13}C$ values were derived from a range of fine-grained to coarse-grained lithologies that make up the individual Siluro–Devonian sections sampled in West Virginia, Nevada and Oklahoma. Micritic components were preferentially drilled from fresh rock surfaces, although most samples included heterogeneous admixtures of skeletal components (i.e. brachiopod, crinoid and bryozoan fragments) and minor calcite cements. Despite potential pitfalls (e.g. organic matter oxidation, 'vital effects'), there is good reason to believe that primary seawater $\delta^{13}C$ values are commonly obtained from what are essentially bulk-rock analyses. Several authors have demonstrated that $\delta^{13}C$ values are largely rock-buffered (i.e. the carbon of the new mineral phase is derived from the old mineral phase) during the diagenetic histories that typically affect marine carbonates (Magaritz, 1983; Banner and Hanson, 1990). For example, an Upper Cambrian (Steptoean Stage) $\delta^{13}C$ excursion of +5‰ has been recorded in a widely varied set of lithofacies on four separate continents (SPICE excursion; Saltz-

man et al., 1998, 2000a), including dolomite facies (Glumac and Walker, 1998). Preservation of secular trends in $\delta^{13}C$ from dominantly micritic limestones of Late Cambrian (Gao and Land, 1991; Ripperdan et al., 1992), Late Ordovician (Finney et al., 1999; Kump et al., 1999), Late Devonian (Joachimski and Buggisch, 1993; Wang et al., 1996) and Early Mississippian age (Saltzman, 2002) has also been demonstrated between widely separated stratigraphic sections. This relative immobility of $\delta^{13}C$ contrasts with $\delta^{18}O$, which is easily reset because of the water-dominated nature of the diagenetic reactions.

Brachiopod shells made up of low-Mg calcite are often considered the most reliable component for chemostratigraphic investigations and indeed have yielded consistent $\delta^{13}C$ results from stratigraphic intervals on separate continents (e.g. carboniferous studies in Mii et al., 1999; Bruckschen et al., 1999). However, brachiopods are not available for the construction of continuous, high-resolution $\delta^{13}C$ curves in significant portions of the Siluro–Devonian transition targeted in this study, particularly the Roberts Mountains Formation of Nevada. It is encouraging that $\delta^{13}C$ values from Silurian micritic limestones generally overlap the ranges of brachiopod calcite analyzed from the same formations. For example, micrites and bulk-rock analyses from Silurian sections in northern Europe (Kaljo et al., 1997; Wigforss-Lange, 1999) faithfully record the major positive $\delta^{13}C$ excursions that have been recognized in brachiopod calcite (Wenzel and Joachimski, 1996; Azmy et al., 1998), and these events have subsequently been traced into parts of North America using fine-grained carbonate components (Saltzman, 2001).

All carbonate samples were roasted under vacuum at 380°C for 1 h to remove volatile contaminants prior to analysis. Carbonate powders were reacted with 100% phosphoric acid at 75°C in an online carbonate preparation line (Carbo–Kiel – single sample acid bath) connected to a Finnigan Mat 251 or 252 mass spectrometer. All isotope ratios are reported in per mil relative to the VPDB standard. Measured precision for $\delta^{13}C$ and $\delta^{18}O$ was maintained at better than 0.1‰.

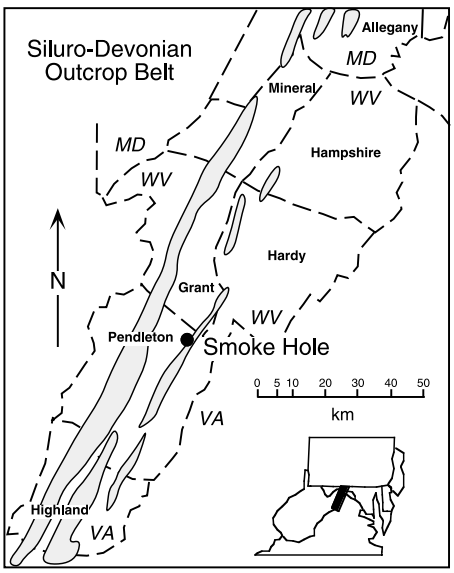

Fig. 2. Silurian–Devonian outcrop map and position of the Smoke Hole section sampled for carbon isotopes in West Virginia, after Helfrich (1978).

4. Results

4.1. Smoke Hole, eastern West Virginia

A section of the Helderberg Group was sampled in a roadcut exposure along the Smoke Hole River in eastern West Virginia (Fig. 2), where the succession attains near its maximum thickness of ~140 m (Dorobek and Read, 1986). At Smoke Hole, the Keyser Limestone marks the lowest formation within the Helderberg and conformably overlies the Tonoloway Limestone, a sequence of sparsely fossiliferous, laminated lime mudstones (Fig. 3). The Keyser is made up primarily of argillaceous, nodular wackestone and skeletal packstone facies (~70-m thick) that are further subdivided into upper and lower limestone members and a middle, clastic-dominated unit (Big Mountain Shale). The position of the Silurian–Devonian boundary is constrained to the Upper Keyser Limestone (Fig. 3) by conodont collections containing the last occurrence of *Oulodus elegans* at ~10 m below the top of the

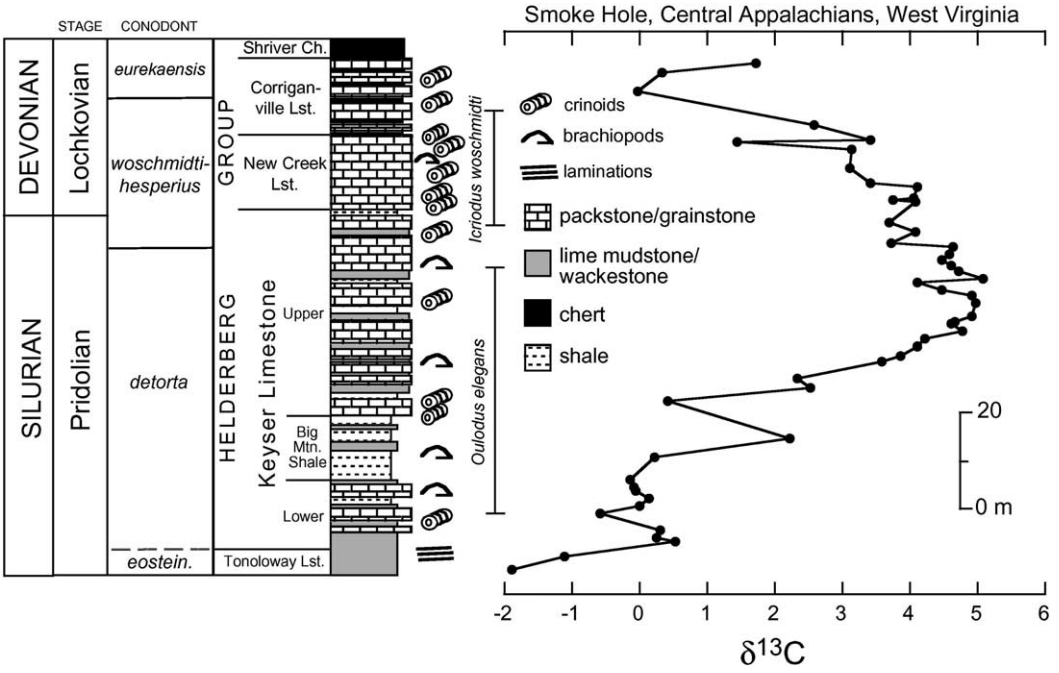

Fig. 3. $\delta^{13}C$ curve and conodont biostratigraphy for the section of the Helderberg Group at Smoke Hole, West Virginia (see Table 1). Conodont zonation based on Helfrich (1978) and Denkler and Harris (1988). Position of the *eurekaensis* zone within the Helderberg is inferred from Sartain (1981).

formation, and a collection yielding the first occurrence of *Icriodus woschmidti* at ~3 m below the top (Helfrich, 1978; Denkler and Harris, 1988). The contact between the Keyser and New Creek Limestone is gradational at Smoke Hole and drawn at the base of the lowest interval of thick-bedded crinoidal packstone to grainstone. The New Creek grades into cherty wackestones of the overlying Corriganville Limestone, and sampling of carbonates was halted at the top of the Corriganville where the siliceous facies of the Shriver Chert begin to dominate.

Carbon isotope ($\delta^{13}C$) values rise gradually from a low near −1‰ in the uppermost Tonoloway Limestone, to a peak near +5‰ in the Upper Keyser Limestone (Fig. 3; Table 1). $\delta^{13}C$ values remain high (≥ +4‰) across the Silurian–Devonian (Pridolian-Lochkovian) boundary drawn just above the first occurrence of the conodont *I. woschmidti*, before beginning to fall toward pre-excursion values ≤ +1‰ in the lower part of the Corriganville Limestone.

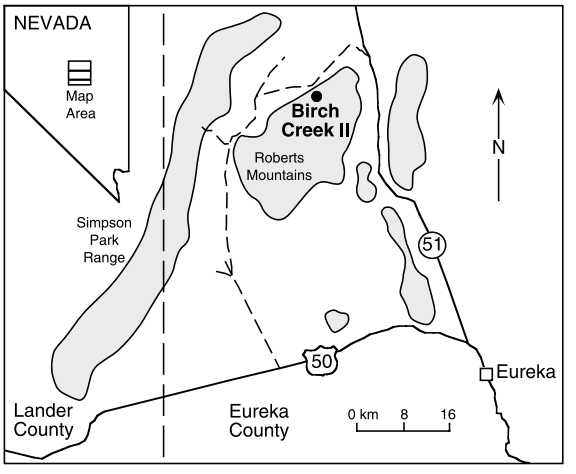

Fig. 4. Locality map for the Birch Creek II section sampled for carbon isotopes in the Roberts Mountains of central Nevada (after Klapper and Murphy, 1975). The Lower Devonian section sampled in the Northern Antelope Range (included in Fig. 5) is ~70 km to the south of the Birch Creek section.

Table 1
Stable isotope data, Smoke Hole, West Virginia

Meter[a]	$\delta^{13}C$	$\delta^{18}O$	Conodont zone	Stage	Formation
0.0	−1.91	−8.03	*eostein.* or *detorta*	Pridolian	Tonoloway
2.5	−1.11	−7.71	*eostein.* or *detorta*	Pridolian	Tonoloway
5.5	0.52	−6.59	*detorta*	Pridolian	Lower Keyser
6.5	0.23	−7.06	*detorta*	Pridolian	Lower Keyser
8.0	0.30	−7.47	*detorta*	Pridolian	Lower Keyser
11.5	−0.58	−7.21	*detorta*	Pridolian	Lower Keyser
13.0	0.00	−7.39	*detorta*	Pridolian	Lower Keyser
14.5	0.13	−7.32	*detorta*	Pridolian	Lower Keyser
16.0	−0.07	−7.26	*detorta*	Pridolian	Lower Keyser
17.0	−0.09	−7.18	*detorta*	Pridolian	Lower Keyser
18.5	−0.16	−7.39	*detorta*	Pridolian	Big Mtn. Shale
23.0	0.21	−6.79	*detorta*	Pridolian	Big Mtn. Shale
27.0	2.21	−4.87	*detorta*	Pridolian	Big Mtn. Shale
35.0	0.40	−6.58	*detorta*	Pridolian	Upper Keyser
37.7	2.51	−6.02	*detorta*	Pridolian	Upper Keyser
39.7	2.32	−6.25	*detorta*	Pridolian	Upper Keyser
43.2	3.58	−6.80	*detorta*	Pridolian	Upper Keyser
44.2	3.85	−6.95	*detorta*	Pridolian	Upper Keyser
46.2	4.10	−6.21	*detorta*	Pridolian	Upper Keyser
47.7	4.21	−6.36	*detorta*	Pridolian	Upper Keyser
49.2	4.76	−5.47	*detorta*	Pridolian	Upper Keyser
50.7	4.60	−6.00	*detorta*	Pridolian	Upper Keyser
51.2	4.67	−5.74	*detorta*	Pridolian	Upper Keyser
52.2	4.92	−6.23	*detorta*	Pridolian	Upper Keyser
55.2	4.96	−6.50	*detorta*	Pridolian	Upper Keyser
56.7	4.90	−5.75	*detorta*	Pridolian	Upper Keyser
57.7	4.47	−6.41	*detorta*	Pridolian	Upper Keyser
59.2	4.09	−4.90	*detorta*	Pridolian	Upper Keyser
60.2	5.07	−5.39	*detorta*	Pridolian	Upper Keyser
61.7	4.71	−6.44	*detorta*	Pridolian	Upper Keyser
62.7	4.61	−5.84	*detorta*	Pridolian	Upper Keyser
64.2	4.46	−6.71	*detorta*	Pridolian	Upper Keyser
65.2	4.57	−6.98	*detorta*	Pridolian	Upper Keyser
66.7	4.64	−6.52	*detorta*	Pridolian	Upper Keyser
67.7	3.72	−6.50	*hesperius (woschm.)*	Pridolian	Upper Keyser
69.7	4.06	−6.54	*hesperius (woschm.)*	Pridolian	Upper Keyser
71.7	3.69	−6.25	*hesperius (woschm.)*	Pridolian	Upper Keyser
76.0	4.08	−6.43	*hesperius (woschm.)*	Lochkovian	New Creek
76.5	3.73	−6.68	*hesperius (woschm.)*	Lochkovian	New Creek
77.0	4.05	−6.61	*hesperius (woschm.)*	Lochkovian	New Creek
79.0	4.09	−6.04	*hesperius (woschm.)*	Lochkovian	New Creek
80.0	3.42	−6.31	*hesperius (woschm.)*	Lochkovian	New Creek
83.0	3.10	−6.34	*hesperius (woschm.)*	Lochkovian	New Creek
87.0	3.13	−6.37	*hesperius (woschm.)*	Lochkovian	New Creek
88.5	1.43	−6.24	*hesperius (woschm.)*	Lochkovian	New Creek
89.0	3.40	−6.13	*hesperius (woschm.)*	Lochkovian	New Creek
92.0	2.56	−6.14	*hesperius (woschm.)*	Lochkovian	Corriganville
99.0	−0.03	−6.29	*eurekaensis*	Lochkovian	Corriganville
103.0	0.31	−5.90	*eurekaensis*	Lochkovian	Corriganville
105.0	1.72	−5.43	*eurekaensis*	Lochkovian	Corriganville

[a] Section begins 3.3 meters below the top of the Tonoloway Limestone.

4.2. Roberts Mountains and Northern Antelope Range, central Nevada

An upper Pridolian through lowermost Lochkovian section of the Roberts Mountains Formation is exposed along Birch Creek in the Roberts Mountains of central Nevada (Fig. 4; Berry and Murphy, 1975; Klapper and Murphy, 1975). The upper part of the Roberts Mountains Formation at the Birch Creek II section (Fig. 5) consists of alternating marl stone, lime mudstone and wackestone lithologies, with minor intervals of skeletal packstone and pebbly limestone lithologies. The position of the Silurian–Devonian boundary is constrained by conodont collections containing the last occurrence of *Ozarkodina eosteinhornensis* at ~170 m above the base of the Birch Creek II section (indicating a late Silurian age), and the first occurrence of *I. woschmidti* at 171 m (Klapper and Murphy, 1975). In addition, the first occurrence of the graptolite *M. uniformis*, which defines the Silurian–Devonian boundary at the Klonk GSSP, is at 173 m above the base of the Birch Creek II section (Berry and Murphy, 1975). A significant covered interval occurs at Birch Creek ~25 m above the Silurian–Devonian boundary (Fig. 5), and the remainder of the Lochkovian samples analyzed come from a section of the Lone Mountain Dolomite exposed in the Northern Antelope Range ~70 km to the south of the Roberts Mountains. The Lone Mountain Dolomite in the Northern Antelope Range consists of an essentially monofacial succession of dolomicrites that have yielded an upper Lochko-

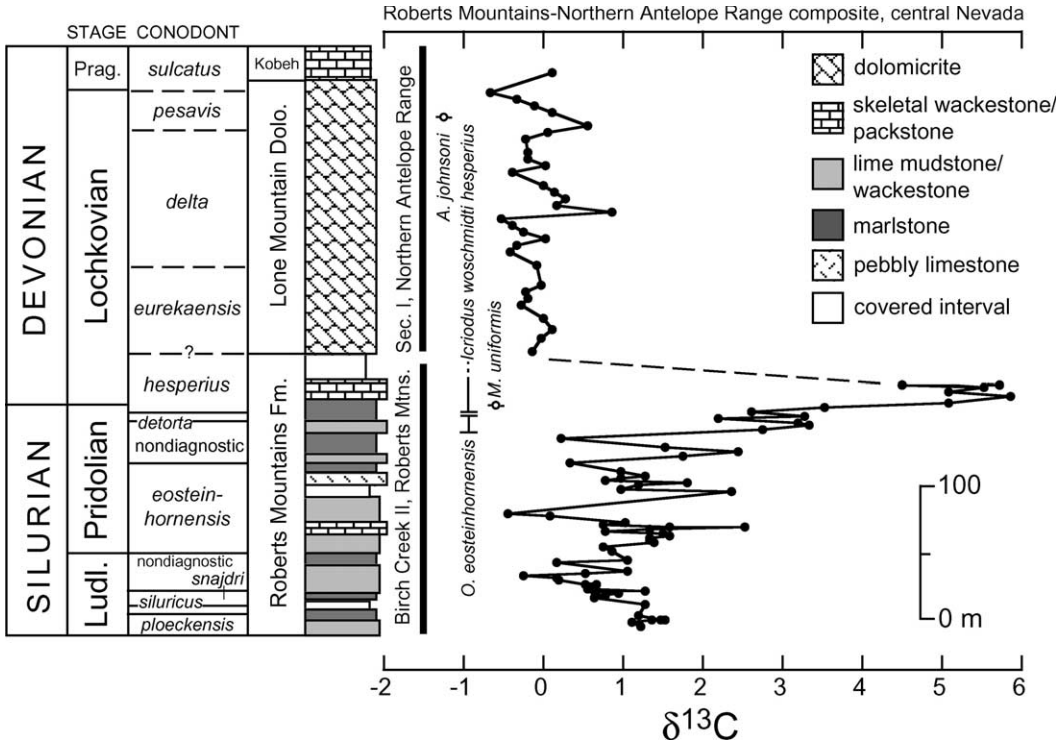

Fig. 5. $\delta^{13}C$ curve and conodont biostratigraphy (Klapper and Murphy, 1975) for the Pridolian to Lochkovian Roberts Mountains Formation at the Birch Creek II section in the Roberts Mountains, central Nevada (Matti and McKee, 1977); and the Lochkovian to Pragian section of the Lone Mountain Dolomite in the Northern Antelope Range of central Nevada (see Table 2). The first occurrence of the graptolite *M. uniformis* at Birch Creek II (Berry and Murphy, 1975) marks the Silurian–Devonian boundary. The top of the sampled portion of the Roberts Mountains Formation at Birch Creek II is a covered interval, and the precise correlation with the base of the sparsely fossiliferous Lone Mountain Dolomite section sampled in the Northern Antelope Range is uncertain (Johnson and Murphy, 1984).

Table 2
Stable isotope data, Central Nevada

Meter[a]	$\delta^{13}C$	$\delta^{18}O$	Conodont zone	Section	Meter[a]	$\delta^{13}C$	$\delta^{18}O$	Conodont zone	Section
9.8	1.22	−13.00	*ploeckensis*	BC II	138.7	1.75	−7.00	non-diagnostic	BC II
12.8	1.11	−9.47	*ploeckensis*	BC II	142.0	2.43	−7.74	non-diagnostic	BC II
15.2	1.34	−13.10	*ploeckensis*	BC II	144.8	1.53	−6.81	non-diagnostic	BC II
15.5	1.52	−11.08	*ploeckensis*	BC II	152.4	0.21	−7.75	non-diagnostic	BC II
15.8	1.47	−8.85	*ploeckensis*	BC II	159.1	2.73	−5.22	*eostein./detorta*	BC II
18.0	1.17	−13.40	*ploeckensis*	BC II	161.8	3.31	−10.02	*eostein./detorta*	BC II
26.5	1.26	−11.42	non-diagnostic	BC II	163.4	3.19	−10.24	*eostein./detorta*	BC II
31.4	0.62	−10.11	*latialata (snajdri)*	BC II	166.1	2.17	−12.76	*eostein./detorta*	BC II
32.6	0.78	−11.48	*latialata (snajdri)*	BC II	168.6	3.27	−8.64	*eostein./detorta*	BC II
33.2	0.67	−11.83	*latialata (snajdri)*	BC II	172.2	2.61	−14.09	*hesperius*	BC II
34.7	0.93	−11.05	*latialata (snajdri)*	BC II	175.3	3.52	−11.98	*hesperius*	BC II
36.0	0.64	−11.15	*latialata (snajdri)*	BC II	179.2	5.08	−6.46	*hesperius*	BC II
37.5	1.27	−16.37	non-diagnostic	BC II	182.6	5.84	−4.19	*hesperius*	BC II
39.0	0.55	−12.44	non-diagnostic	BC II	186.5	5.08	−8.43	*hesperius*	BC II
40.5	0.57	−10.63	non-diagnostic	BC II	189.6	5.52	−5.88	*hesperius*	BC II
40.8	0.61	−10.52	non-diagnostic	BC II	191.1	4.49	−13.17	*hesperius*	BC II
42.1	0.66	−12.29	non-diagnostic	BC II	192.0	5.72	−5.04	*hesperius*	BC II
42.4	0.52	−12.11	non-diagnostic	BC II	217.0	−0.15	−4.80	non-diagnostic	NA I
44.8	0.18	−9.94	non-diagnostic	BC II	227.0	−0.05	−2.52	non-diagnostic	NA I
46.3	0.16	−8.92	non-diagnostic	BC II	234.0	0.09	−3.08	non-diagnostic	NA I
47.9	−0.27	−10.05	non-diagnostic	BC II	242.0	−0.01	−4.01	non-diagnostic	NA I
49.4	0.52	−13.28	non-diagnostic	BC II	251.0	−0.30	−2.45	non-diagnostic	NA I
51.5	1.05	−9.44	non-diagnostic	BC II	256.0	−0.19	−0.20	non-diagnostic	NA I
58.5	0.16	−7.49	non-diagnostic	BC II	262.0	−0.23	−1.65	non-diagnostic	NA I
60.0	1.05	1.11	non-diagnostic	BC II	267.0	−0.03	−0.89	non-diagnostic	NA I
67.1	0.86	−12.90	non-diagnostic	BC II	282.0	−0.08	−2.77	non-diagnostic	NA I
70.1	0.73	−12.64	*P. index (eostein.)*	BC II	292.0	−0.42	−3.01	non-diagnostic	NA I
73.8	1.37	−17.60	*P. index (eostein.)*	BC II	297.0	−0.33	−3.43	non-diagnostic	NA I
75.3	1.31	−13.63	*P. index (eostein.)*	BC II	302.0	0.03	−2.93	non-diagnostic	NA I
76.8	1.31	−12.18	*P. index (eostein.)*	BC II	307.0	−0.26	−1.93	non-diagnostic	NA I
78.3	1.58	−11.75	*P. index (eostein.)*	BC II	312.0	−0.39	−4.33	non-diagnostic	NA I
79.9	1.48	−11.13	*P. index (eostein.)*	BC II	317.0	−0.54	−2.54	non-diagnostic	NA I
81.7	0.78	−8.94	*P. index (eostein.)*	BC II	322.0	0.84	−3.51	non-diagnostic	NA I
83.2	1.33	−12.83	*P. index (eostein.)*	BC II	327.0	0.15	−2.19	non-diagnostic	NA I
84.4	2.51	−7.27	*P. index (eostein.)*	BC II	332.0	0.26	−3.00	non-diagnostic	NA I
85.3	1.57	−11.94	*P. index (eostein.)*	BC II	337.0	0.13	−2.11	non-diagnostic	NA I
87.2	0.74	−15.12	*P. index (eostein.)*	BC II	342.0	−0.02	−2.22	non-diagnostic	NA I
88.7	1.01	−9.88	*P. index (eostein.)*	BC II	352.0	−0.39	−3.64	non-diagnostic	NA I
93.0	0.06	−5.28	*P. index (eostein.)*	BC II	357.0	0.02	−1.82	non-diagnostic	NA I
94.5	−0.45	−10.92	*P. index (eostein.)*	BC II	362.0	−0.20	−2.28	non-diagnostic	NA I
111.3	2.34	−6.67	*P. index (eostein.)*	BC II	367.0	−0.20	−3.56	non-diagnostic	NA I
112.8	0.97	−10.85	*P. index (eostein.)*	BC II	377.0	−0.23	−2.98	non-diagnostic	NA I
117.3	1.18	−7.36	*P. index (eostein.)*	BC II	382.0	0.05	0.01	non-diagnostic	NA I
118.9	1.79	−7.48	*P. index (eostein.)*	BC II	387.0	0.55	0.39	*delta* or *pesavis*	NA I
120.4	0.77	−8.71	*P. index (eostein.)*	BC II	397.0	0.09	−2.61	*delta* or *pesavis*	NA I
121.0	0.95	−14.07	*P. index (eostein.)*	BC II	402.0	−0.12	−3.03	*delta* or *pesavis*	NA I
123.4	1.26	−6.74	*P. index (eostein.)*	BC II	407.0	−0.35	−3.26	*delta* or *pesavis*	NA I
126.5	0.95	−6.12	*P. index (eostein.)*	BC II	412.0	−0.69	−3.28	*pesav.* or *sulcat.*	NA I
132.6	0.32	−6.97	*P. index (eostein.)*	BC II	427.0	0.10	−0.59	*sulcatus*	NA I

[a] Section at Birch Creek (BC II) begins at base of the Roberts Mountains Formation (see Klapper and Murphy, 1975); section at Northern Antelope Range (NAI) begins 209 meters below the top of the Lone Mountain Dolomite (see Trojan, 1978; Johnson and Murphy, 1984).

vian (*delta* or *pesavis* zone) conodont fauna from 33.5 m below the top of the formation (Johnson and Murphy, 1984).

$\delta^{13}C$ values begin near +1‰ in the lower part of the Roberts Mountains Formation at Birch Creek II (Fig. 3; Table 2) and rise gradually to heavier values through a series of higher-frequency fluctuations ($\geq \pm 2$‰), ultimately reaching a distinct peak of +5.8‰ at the top of the section, ~20 m above the level of the Silurian–Devonian boundary. The Lochkovian succession of the Lone Mountain Dolomite from the Northern Antelope Range shows relatively uniform $\delta^{13}C$ values near −1‰.

4.3. Arbuckle Mountains, south-central Oklahoma

The I-35 roadcut and supplementary section at Highway 77 in the Arbuckle Mountains of south-central Oklahoma (Fig. 6; Saltzman, 2001) provide nearly complete exposures of Silurian–Devonian transition in the upper Henryhouse and lower Haragan formations of the Hunton Group. Both the Henryhouse and Haragan are comprised of similar marl stone and lime mudstone to wackestone-dominated sequences, and the formational contact is drawn based on biostratigraphic evidence at the I-35 section (Amsden, 1962, 1988). However, in other parts of the Oklahoma Basin, evidence exists for relief on the Henryhouse–Haragan surface, and Amsden (1988) has suggested that a substantial sedimentary hiatus may be present. The Silurian–Devonian boundary at the I-35 section can be narrowed to within a thin, zonally indeterminate interval (~0.5 m) based on collections containing *Oulodus elegans detorta* from near the top of the Henryhouse Formation (sample 2BB, Fig. 7), and *Icriodus postwoschmidti* just above the base of the Haragan Formation (sample 2E; *eurekaensis* zone of Barrick and Klapper, 1992). The lack of evidence for the diagnostic conodont *I. woschmidti* (which occurs within meters of the first occurrence of the graptolite *M. uniformis* and the Silurian–Devonian boundary at the GSSP at Klonk and the Birch Creek II section in Nevada; Fig. 5) in this interval is consistent with the notion of a hiatus corresponding to the *hesperius* (*woschmidti*) conodont zone (uppermost Pridoli and lowermost Lochkovian).

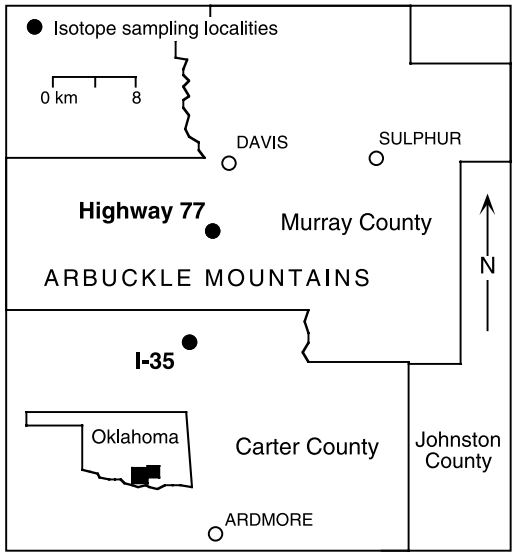

Fig. 6. Locality map for the I-35 and Highway 77 sections sampled for carbon isotopes in the Arbuckle Mountains of southern Oklahoma after Barrick and Klapper (1992).

$\delta^{13}C$ values rise from +1‰ in the middle and upper portions of the Henryhouse Formation at the Highway 77 section (*eosteinhornensis* and *detorta* zones; Saltzman, 2001) to a maximum near +2‰ at the top of the formation and ~0.5 m above the sample containing a latest Pridolian conodont fauna (Fig. 7 Table 3). $\delta^{13}C$ values in the basal Haragan Formation reach a maximum of $\geq$+3‰ in the *eurekaensis* zone, before falling gradually to a pre-excursion baseline of ~0‰ at the top of the Haragan.

5. Discussion

5.1. Correlation of the Silurian–Devonian $\delta^{13}C$ excursion

The Silurian–Devonian transition is marked by a positive $\delta^{13}C$ shift in the three Euramerican sections investigated (Figs. 3, 5, 7). The maximum $\delta^{13}C$ value reached is +5.8‰ within the lowermost Lochkovian *hesperius* conodont zone at the Birch Creek II section in central Nevada. The carbon isotope trends in Euramerica can be cor-

related using conodont and graptolites with a $\delta^{13}C$ shift spanning the Silurian–Devonian boundary in several Gondwanan sections, including the GSSP at Klonk in the Czech Republic (Fig. 8; Hladikova et al., 1997; Buggisch, 2001) and the well-dated section at Cellon in the Carnic Alps (Schonlaub et al., 1994). In addition, $\delta^{13}C$ data from strata of the *hesperius* zone in the Jack Limestone of Queensland, Australia (Andrew et al., 1994) also show a large positive anomaly ($\geq +6‰$), and argue against the $\delta^{13}C$ shift being purely an artifact of diagenesis, which is unlikely to shift $\delta^{13}C$ to such heavy values simultaneously in distant paleotectonic and paleogeographic settings (Fig. 1). The results of this study provide the first evidence for a global scale perturbation in carbon cycling during the Silurian–Devonian transition, signaled by one of the largest $\delta^{13}C$ peaks known thus far in the Paleozoic (e.g. compare with a shift of $\geq +6‰$ known from the Late Ordovician in Kump et al., 1999; and $\geq +5‰$ for the Upper Cambrian in Saltzman et al., 2000a).

The biostratigraphic basis for correlation of $\delta^{13}C$ peaks between Euramerica and Gondwana, including the Klonk GSSP, is most firmly established in the Birch Creek II section (Fig. 5) of Nevada, where a sequence of shared and independent faunal events delineate the Silurian–Devonian boundary interval (Klapper and Murphy, 1975). These events include the overlap in the range of the conodonts *Ozarkodina remsheidensis eosteinhornensis* and *O. remsheidensis remsheidensis*, indicating a latest Silurian age, and the first occurrences of the conodont *I. woschmidti* and the graptolite *M. uniformis* ~2 m higher in the section. Correlation of the $\delta^{13}C$ peak at the Smoke Hole section in the Appalachian Basin (Fig. 3) is based on strata that record the first occurrence of the cosmopolitan conodont *I. woschmidti* above the last occurrence of *O. elegans*, although it

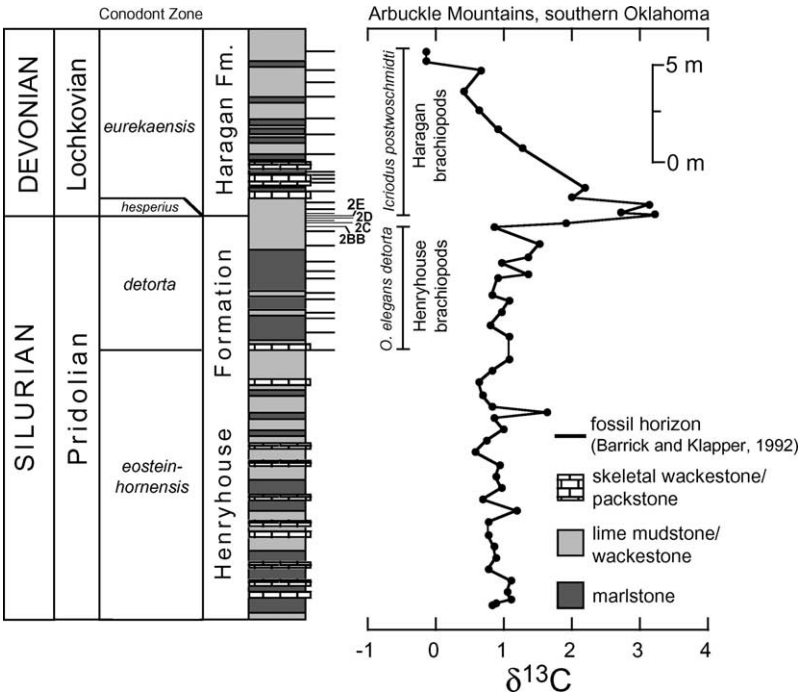

Fig. 7. Integrated $\delta^{13}C$ and conodont biostratigraphy (Barrick and Klapper, 1976, 1992) for the Pridolian Henryhouse and Lochkovian Haragan formations in the Arbuckle Mountains, south-central Oklahoma (see Table 3). Fossil horizons are plotted for the I-35 section and numbered for key collections used to delineate the Silurian–Devonian boundary and inferred hiatus which removes the *hesperius* zone (see Barrick and Klapper, 1992), and thus likely a portion of the larger ($\geq +5‰$) $\delta^{13}C$ excursion seen in Nevada and West Virginia. The abrupt change in brachiopod faunas between the Henryhouse and Haragan formations (see Amsden, 1988) is from Barrick and Klapper (1992).

Table 3
Stable isotope data, Arbuckle Mountains, Oklahoma

Meter[a]	$\delta^{13}C$	$\delta^{18}O$	Conodont zone	Section (#)[b]	Stage	Formation
0.0	0.82	−4.13	*eosteinhornensis*	Highway 77	Pridolian	Henryhouse
0.1	0.88	−4.53	*eosteinhornensis*	Highway 77	Pridolian	Henryhouse
0.3	1.10	−4.10	*eosteinhornensis*	Highway 77	Pridolian	Henryhouse
0.6	1.05	−4.34	*eosteinhornensis*	Highway 77	Pridolian	Henryhouse
1.2	1.11	−4.03	*eosteinhornensis*	Highway 77	Pridolian	Henryhouse
1.8	0.78	−4.37	*eosteinhornensis*	Highway 77	Pridolian	Henryhouse
2.4	0.87	−4.19	*eosteinhornensis*	Highway 77	Pridolian	Henryhouse
3.0	0.85	−3.72	*eosteinhornensis*	Highway 77	Pridolian	Henryhouse
3.6	0.76	−4.44	*eosteinhornensis*	Highway 77	Pridolian	Henryhouse
4.2	0.78	−4.13	*eosteinhornensis*	Highway 77	Pridolian	Henryhouse
4.8	1.18	−4.21	*eosteinhornensis*	Highway 77	Pridolian	Henryhouse
5.4	0.68	−4.24	*eosteinhornensis*	Highway 77	Pridolian	Henryhouse
6.0	0.96	−4.01	*eosteinhornensis*	Highway 77	Pridolian	Henryhouse
6.6	0.88	−4.10	*eosteinhornensis*	Highway 77 (338a)	Pridolian	Henryhouse
7.2	0.93	−4.29	*eosteinhornensis*	Highway 77	Pridolian	Henryhouse
7.8	0.58	−3.82	*eosteinhornensis*	Highway 77	Pridolian	Henryhouse
8.4	0.75	−4.56	*eosteinhornensis*	Highway 77	Pridolian	Henryhouse
9.0	0.99	−4.11	*eosteinhornensis*	Highway 77 (342)	Pridolian	Henryhouse
9.6	0.84	−4.40	*eosteinhornensis*	Highway 77 (343)	Pridolian	Henryhouse
9.9	1.64	−4.66	*eosteinhornensis*	Highway 77	Pridolian	Henryhouse
10.2	0.82	−3.81	*eosteinhornensis*	Highway 77	Pridolian	Henryhouse
10.8	0.69	−4.02	*eosteinhornensis*	Highway 77	Pridolian	Henryhouse
11.4	0.64	−4.40	*eosteinhornensis*	Highway 77	Pridolian	Henryhouse
12.0	0.83	−3.85	*detorta*	Highway 77	Pridolian	Henryhouse
12.6	1.06	−4.27	*detorta*	Highway 77	Pridolian	Henryhouse
13.8	1.06	−3.78	*detorta*	Highway 77	Pridolian	Henryhouse
14.4	0.81	−4.48	*detorta*	Highway 77	Pridolian	Henryhouse
15.0	0.96	−4.21	*detorta*	Highway 77	Pridolian	Henryhouse
15.6	1.07	−4.01	*detorta*	Highway 77	Pridolian	Henryhouse
15.9	0.83	−4.23	*detorta*	Highway 77	Pridolian	Henryhouse
16.8	0.92	−4.49	*detorta*	Highway 77 (40 a)	Pridolian	Henryhouse
17.0	1.36	−3.80	*detorta*	I-35	Pridolian	Henryhouse
17.6	0.97	−3.53	*detorta*	I-35	Pridolian	Henryhouse
17.9	1.36	−4.11	*detorta*	I-35	Pridolian	Henryhouse
18.5	1.53	−3.72	*detorta*	I-35	Pridolian	Henryhouse
19.4	0.84	−2.89	*detorta*	I-35 (2BB)	Pridolian	Henryhouse
19.6	1.92	−3.56	non-diagnostic	I-35 (2C)	Lochkovian?	Henryhouse
20.1	3.22	−3.40	*postwoschmidti*	I-35 (2E)	Lochkovian	Haragan
20.2	2.70	−3.28	*postwoschmidti*	I-35 (3)	Lochkovian	Haragan
20.6	3.12	−3.48	*postwoschmidti*	I-35	Lochkovian	Haragan
21.0	2.00	−3.35	*postwoschmidti*	I-35	Lochkovian	Haragan
21.5	2.18	−3.03	*postwoschmidti*	I-35 (4)	Lochkovian	Haragan
23.5	1.26	−3.01	*postwoschmidti*	I-35	Lochkovian	Haragan
24.5	0.92	−2.98	*postwoschmidti*	I-35	Lochkovian	Haragan
25.5	0.63	−3.04	*postwoschmidti*	I-35	Lochkovian	Haragan
26.5	0.41	−3.33	*postwoschmidti*	I-35	Lochkovian	Haragan
27.5	0.67	−2.91	*postwoschmidti*	I-35	Lochkovian	Haragan
27.5	−0.14	−3.20	*postwoschmidti*	I-35	Lochkovian	Haragan
28.5	−0.14	−3.38	*postwoschmidti*	I-35	Lochkovian	Haragan

[a] Section begins at 7.6 meters above the base of the Henryhouse Formation at Highway 77 (see Barrick and Klapper, 1976; Saltzman, 2001).

[b] Numbers are from Barrick and Klapper (1992) for I-35 section; and Barrick and Klapper (unpublished) for Highway 77 section.

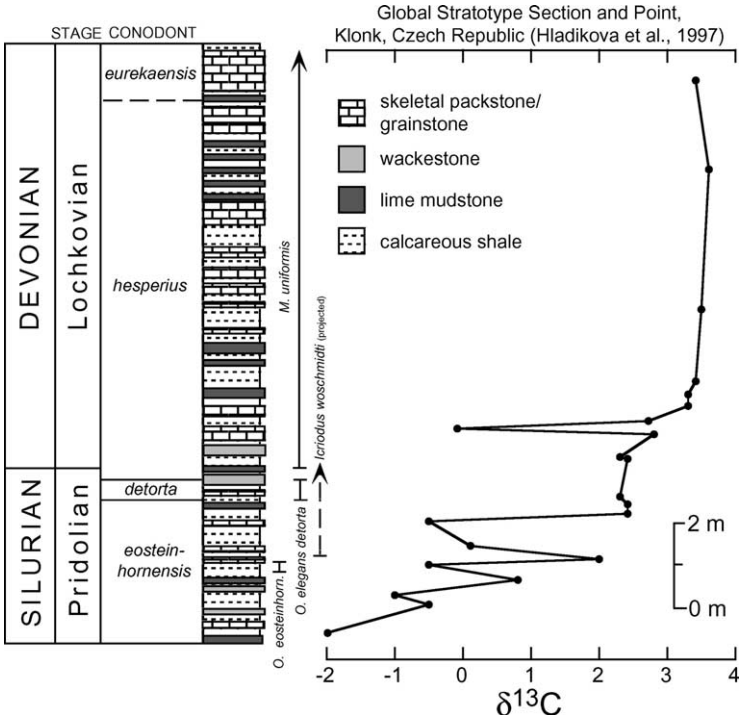

Fig. 8. Plot of $\delta^{13}C$ (from Hladikova et al., 1997) and conodont biostratigraphy (Jeppsson, 1989; Chlupac and Hladil, 2000) for the Klonk GSSP in the Czech Republic. The Silurian–Devonian boundary is defined by the first occurrence of the graptolite *M. uniformis*, and the occurrence of *I. woschmidti* is projected from a nearby section in the Prague Basin (Jeppsson, 1988, 1989; Chlupac and Hladil, 2000).

should be noted that peak $\delta^{13}C$ values are reached ~5 m below the top of the latest Pridolian *detorta* zone here, which is somewhat older than at Birch Creek II (~20 m above the base of the first occurrence of the Lochkovian graptolite *M. uniformis*) or Klonk (~7 m above the base of the first occurrence of *M. uniformis*). This offset in $\delta^{13}C$ peaks between Smoke Hole and Birch Creek II could be explained if the conodont species *O. elegans* ranged into the earliest Lochkovian in the Appalachian Basin.

At the I-35 section in south-central Oklahoma, the Silurian–Devonian transition contains a significant hiatus between the last occurrence of *O. elegans* and the first occurrence of *I. postwoschmidti* (which can be tied into the middle part of the *uniformis* graptolite zone at Klonk), corresponding to at least a part of the *hesperius* zone and possibly including parts of the underlying and overlying zones (Barrick and Klapper, 1992). Consistent with the conodont biostratigraphy, the beginning of the positive $\delta^{13}C$ shift is truncated at the top of the Henryhouse Formation (Fig. 7), and only a portion of the falling limb of the excursion (from maximum values of +3‰ to a baseline near 0‰) can be seen in the lowermost few meters of the Haragan Formation of *eurekaensis* zone age. Alternatively, it may be that a condensed interval at the top of the Henryhouse Formation in the Oklahoma Basin has obscured the complete record of the +5‰ $\delta^{13}C$ excursion recorded elsewhere in North America, although no evidence for condensation (i.e. phosphatized grains or glauconite) has been observed.

5.2. Mechanisms for Silurian–Devonian $\delta^{13}C$ excursion

Fluctuations in the $\delta^{13}C$ of marine carbonates that persist on time scales longer than ~10^5 years provide a record of changes in the burial ratio of

organic carbon to carbonate carbon, and may also reflect changes in carbonate weathering rates or the sensitivity of the photosynthetic carbon isotope effect to changes in $pCO2$ (Kump and Arthur, 1999). The steady-state carbon isotopic mass–balance equation most often used to interpret changes in $\delta^{13}C$ of marine carbonates can be represented as:

$$f_{org} = \frac{\delta_w - \delta_{carb}}{\Delta_B}$$

Using this expression (Kump and Arthur, 1999), the organic carbon burial fraction (f_{org}) can be calculated directly from the $\delta^{13}C$ of marine carbonates (δ_{carb}) by assuming constant values for the riverine weathering flux (δ_w) and the magnitude of the photosynthetic carbon isotope effect (Δ_B). Using the Phanerozoic average values of $\delta_w = -5‰$ and constant $\Delta_B = 30‰$ from Kump and Arthur (1999), a shift from +1‰ to +6‰ across the Silurian–Devonian boundary corresponds to an $\sim$83% increase in f_{org}. It is also possible to calculate that $\sim 8.3 \times 10^{18}$ moles of excess carbon had to be buried somewhere in the global oceans during the estimated 1-million-year duration of this 83% increase in f_{org} by substituting average values for the carbon fluxes that make up the long-term carbon cycle at steady-state (values in Kump and Arthur, 1999 as follows: 5×10^{19} moles C/Myr for the riverine input, and 0.2 for f_{org}). The magnitude of the change in f_{org} is, however, very much dependent upon whether pCO_2 (and thus Δ_B) changed significantly during the course of the $\delta^{13}C$ excursion. For example, if the burial of organic carbon caused a reduction in pCO_2 and a decrease in Δ_B (Kump and Arthur, 1999), the $\delta^{13}C$ of organic matter would record a larger positive excursion (and later in time) than δ_{carb} and lead to an underestimation of the magnitude of the increase in f_{org} by using the record of δ_{carb} alone.

As an alternative to the carbon burial hypothesis, it is possible to generate +6‰ peak in δ_{carb} by increasing the $\delta^{13}C$ of the riverine weathering input (δ_w). This may be accomplished by increasing the fraction derived from carbonate weathering (versus isotopically light organic-rich shales) as explored by Kump et al. (1999). These authors have argued that the +6‰ $\delta^{13}C$ shift in Late Ordovician carbonates was due to the effects of global regression on carbonate weathering rates, which increased from 72% to 88% of the total weathering flux during the event (assuming the magnitude of the photosynthetic carbon isotope effect, Δ_B, also increased by $\sim$7‰ in the Late Ordovician). The excess carbonate eroded from exposed platforms during a $\sim$25% increase in the fraction of carbonate weathered is 8×10^{18} mol C, using the steady-state value of 3.6×10^{19} mol C/Myr for the carbonate weathering flux (Kump et al., 1999; Kump and Arthur, 1999).

The record of global organic carbon burial rates and the nature of eustatic sea level changes through the Silurian–Devonian transition are not yet known in sufficient detail to rule out possible scenarios for increasing seawater $\delta^{13}C$ values. This is due in part to the fact that many of the published paleogeographic reconstructions and particularly sea level curves for the Silurian and Devonian systems do not span the boundary itself (e.g. Johnson et al., 1985; Johnson, 1996). Nonetheless, detailed facies analysis of sections in central and southern Europe which have also been analyzed for $\delta^{13}C$ indicates that the Silurian–Devonian transition is marked by a drop in sea level. For example, in the Prague Basin, Kriz (1991) has noted a relatively sharp, regionally persistent contact between deeper-water laminated limestones and the overlying bioclastic crinoidal and cephalopod limestones of the uppermost Pridoli Formation. In the Carnic Alps, a similar facies change from fine-grained nodular limestone to bioclastic limestone occurs several meters below the Silurian–Devonian boundary as defined by the first occurrences of *I. woschmidti* and *M. uniformis* (Flugel et al., 1977). The notion of enhanced weathering during a fall in sea level that spans the Silurian–Devonian transition is supported independently by recent work on magnetosusceptibility at the Klonk GSSP, which shows a positive change interpreted to reflect relatively high accumulation rates of iron and other riverine-derived paramagnetic minerals (Crick et al., 2001).

Evidence that the sea level drop seen in European (Gondwanan) basins during the Silurian–

Devonian transition may be eustatic comes from stratigraphic analysis in the three North American regions that have been investigated for $\delta^{13}C$ in this paper. Among the regions, probably the most detailed sequence stratigraphic and facies reconstruction comes from study of the Helderberg Group and equivalents in the Appalachian Basin, where basin restriction and widespread peritidal to supratidal carbonate deposition during latest Pridolian time reflects regional regression (LaVale Member of the Keyser Limestone in northern West Virginia and Pennsylvania, and time-equivalent Whiteport Dolomite Member of the Rondout Formation in the New Jersey–New York region; Head, 1969; Dorobek and Read, 1986; Denkler and Harris, 1988). Maximum regression is marked by laminated, quartzose, mudcracked dolomicrite within ~5 m of the Silurian–Devonian boundary (defined using the first occurrence of *I. woschmidti*), and is followed by a return to open-marine, subtidal conditions in the early Lochkovian (New Creek Limestone and Coeymans Formation; Denkler and Harris, 1988). A eustatic drop at the Silurian–Devonian boundary is also consistent with evidence in the Oklahoma Basin for a significant biostratigraphic discontinuity (corresponding to all or part of the *hesperius* conodont zone) and regional truncation of underlying Silurian units as discussed by Amsden (1988) and Barrick and Klapper (1992). In central Nevada, the progradation of shallow-water bioclastic limestones of the uppermost Roberts Mountains Formation over laminated lime mudstones and skeletal wackestones of latest Pridolian age may track this same fall in sea level (Klapper and Murphy, 1975; Matti and McKee, 1977).

A eustatic drop during the Silurian–Devonian transition would have exposed older Silurian carbonate units to low-latitude weathering and likely increased the $\delta^{13}C$ of the riverine flux (δ_w). In addition, there are indications that the burial fraction of organic carbon (f_{org}) increased at this time as well. In Gondwana, the development of organic-rich deposits in the Prague Basin and Carnic Alps region during the latest Pridolian and early Lochkovian (Flugel et al., 1977; Schonlaub et al., 1994) has been interpreted to reflect enhanced primary productivity (Hladil, 1991; Buggisch, 2001), perhaps related to increased weathering rates and riverine nutrient fluxes (e.g. Crick et al., 2001). Based on the available evidence, the most plausible scenario for producing the large positive $\delta^{13}C$ excursion in marine carbonates worldwide during the Silurian–Devonian transition involves a combination of increases in organic carbon burial rates (related to increased riverine phosphate delivery rather than enhanced preservation or upwelling) and carbonate weathering.

6. Conclusions

The Silurian–Devonian transition is marked by a significant positive $\delta^{13}C$ shift in the three Euramerican sections investigated in this study. The maximum $\delta^{13}C$ value reached is +5.8‰ at the Birch Creek II section in central Nevada, and this peak can be correlated using conodonts and graptolites with sections in Gondwana, including the GSSP at Klonk in the Prague Basin, and the classical section at Cellon in the Carnic Alps of Austria. The interpretation of the $\delta^{13}C$ excursion at the Silurian–Devonian boundary as recording primary seawater chemistry and representing a global oceanographic event is consistent with the notion of a significant bio-event at that time, affecting several major groups, including the brachiopods and trilobites (Schonlaub, 1986; Boucot, 1990). In addition, this interpretation is in accord with the increasing number of published studies in the Paleozoic that have reported similar carbon isotopic excursions from widely separated stratigraphic sequences and using a range of carbonate components (e.g. Joachimski and Buggisch, 1993; Saltzman et al., 2000a,b; Wang et al., 1996; Azmy et al., 1998; Kump et al., 1999). It would appear that, from a perspective of $\delta^{13}C$ and carbon cycling, the Paleozoic was a particularly volatile period, more like the preceding Neoproterozoic (Kaufman et al., 1991; Hoffman et al., 1998; Saylor et al., 1998) than the last 200 million years of Phanerozoic time. A widely accepted geologic scenario for generating and sustaining these Paleozoic carbon isotope excursions is still forthcoming.

Acknowledgements

J. Barrick provided helpful discussion and guidance to the field area in southern Oklahoma, as well as copies of unpublished biostratigraphic columns. M. Murphy provided guidance in the Roberts Mountains, and discussions with Gil Klapper have been valuable. Students in the Spring 2001 GS 694–Chemostratigraphy course at Ohio State provided assistance with sampling at Smoke Hole, West Virginia. Thoughtful reviews by W.B.N. Berry and C. Underwood improved the manuscript.

References

Amsden, T.W., 1962. Silurian and Early Devonian carbonate rocks of Oklahoma. Am. Assoc. Pet. Geolog. Bull. 46, 1502–1519.

Amsden, T.W., 1988. Late Ordovician through Early Devonian annotated correlation chart and brachiopod range charts for the southern midcontinent region, USA. Okla. Geol. Surv. Bull. 143, 1–53.

Andrew, A.S., Hamilton, P.J., Mawson, R., Talent, J.A., Whitford, D.J., 1994. Isotopic correlation tools in the mid-Paleozoic and their relation to extinction events. Aust. Pet. Explor. Assoc. 34, 268–277.

Azmy, K., Veizer, J., Bassett, M.G., Copper, P., 1998. Oxygen and carbon isotopic composition of Silurian brachiopods: implications for coeval seawater and glaciations. Geol. Soc. Am. Bull. 110, 1499–1512.

Banner, J.L., Hanson, G.N., 1990. Calculation of simultaneous isotopic and trace element variations during water–rock interaction with applications to carbonate diagenesis. Geochim. Cosmochim. Acta 54, 3123–3137.

Barrick, J.E., Klapper, G., 1976. Multielement Silurian (late Llandoverian-Wenlockian) conodonts of the Clarita Formation, Arbuckle Mountains, Oklahoma, and phylogeny of *Kockelella*. Geol. Palaeontol. 10, 59–100.

Barrick, J.E., Klapper, G., 1992. Late Silurian–Early Devonian conodonts from the Hunton Group (upper Henryhouse, Haragan, and Bois d'Arc formations), south-central Oklahoma. Okla. Geol. Surv. Bull. 145, 19–65.

Berdan, J.M., Berry, W.B.N., Boucot, A.J., Cooper, G.A., Jackson, D.E., Johnson, J.G., Klapper, G., Lenz, A.C., Martinsson, A., Oliver, W.A., Rickard, L.V., Thorsteinsson, R., 1969. Siluro–Devonian boundary in North America. Geol. Soc. Am. Bull. 80, 2165–2174.

Berry, W.B.N., Satterfield, I.R., 1972. Late Silurian graptolites from the Bainbridge Formation in southeastern Missouri. J. Paleontol. 46, 492–498.

Berry, W.B.N., Murphy, M.A., 1975. Silurian and Devonian Graptolites of Central Nevada. University of California Publications in Geological Sciences 110, 109 pp.

Borque, P.A., Lesperance, P.J., 1977. Gaspe Peninsula, Quebec. In: Martinsson, A. (Ed.), The Silurian–Devonian Boundary. Int. Union Geol. Sci., Ser. A 5, pp. 245–255.

Boucot, A.J., 1990. Silurian and pre-Upper Devonian bioevents in Extinction events. In: Kauffman, E.G., Walliser, O.H. (Eds.), Earth History, Lecture Notes in Earth Sciences 30. Springer, Berlin, pp. 125–132.

Bruckschen, P., Oesmann, S., Veizer, J., 1999. Isotope stratigraphy of the European Carboniferous: proxy signals for ocean chemistry, climate and tectonics. Chem. Geol. 161, 127–163.

Buggisch, W., 2001. Carbon isotope analysis ($\delta^{13}C$) of Early to Middle Devonian carbonates from the Prague Syncline, the Carnic Alps, and the Montagne Noire (Czech Republic, Austria, France): Geol. Soc. of Am. and Geol. Soc. London, Earth System Processes Meeting, Programmes with Abstracts. Edinburgh, Scotland, 70 pp.

Chlupac, I., Kukal, Z., 1977a. The boundary stratotype at Klonk. In: Martinsson, A. (Ed.), The Silurian–Devonian Boundary. Int. Union Geol. Sci., Ser. A 5, pp. 96–109.

Chlupac, I., Kukal, Z., 1977b. Reflection of possible global Devonian events in the Barrandian area, C.S.S.R. In: Walliser, O.H. (Ed.), Global Bio-Events, Lecture Notes in Earth Sciences 8. Springer, Berlin, pp. 169–179.

Chlupac, I., Hladil, J., 2000. The global stratotype section and point of the Silurian–Devonian boundary. Cour. Forsch.inst. Senckenb. 225, 1–7.

Cowie, J.W., Ziegler, W., Boucot, A.J., Bassett, M.G., Remane, J., 1986. Guidelines and statutes of the international commission on stratigraphy. Cour. Forsch.inst. Senckenb. 83, 1–14.

Crick, R.E., Chlupac, I., El Hassani, A., Ellwood, B.B., Hladil, J., Hrouda, F., 2001. Magnetostratigraphy susceptibility of the Pridolian–Lochkovian (Silurian–Devonian) GSSP (Klonk, Czech Republic) and a coeval sequence in Anti-Atlas Morocco. Palaeogeogr. Palaeoclimatol. Palaeoecol. 167, 73–100.

Denkler, K.E., Harris, A.G., 1988. Conodont-based determination of the Silurian–Devonian boundary in the Valley and Ridge Province, Northern and Central Appalachians. US Geol. Surv. Bull. B 1837, B1–B13.

Dennison, J.M., Head, J.W., 1975. Sealevel variations interpreted from the Appalachian basin Silurian and Devonian. Am. J. Sci. 275, 1089–1120.

Dorobek, S.L., Read, J.F., 1986. Sedimentology and basin evolution of the Siluro–Devonian Helderberg Group, Central Appalachians. J. Sediment. Petrol. 56, 601–613.

Finney, S.C., Berry, W.B.N., Cooper, J.D., Ripperdan, R.L., Sweet, W.C., Jacobson, S.R., Soufiane, A., Achab, A., Noble, P.J., 1999. Late Ordovician mass extinction: a new perspective from stratigraphic sections in central Nevada. Geology 27, 215–218.

Flugel, H.W., Hermann, J., Schonlaub, H.P., Vai, G.B., 1977. Carnic Alps. In: Martinsson, A. (Ed.), The Silurian–Devonian Boundary. Int. Union Geol. Sci., Ser. A 5, pp. 126–142.

Gao, G., Land, L.S., 1991. Geochemistry of Cambrian–Ordovician Arbuckle limestone, Oklahoma: implications for diagenetic $\delta^{18}O$ alteration and secular $\delta^{13}C$ and $^{87}Sr/^{86}Sr$ variation. Geochim. Cosmochim. Acta 55, 2911–2920.

Glumac, B., Walker, K.R., 1998. A Late Cambrian positive carbon-isotope excursion in the southern Appalachians: relation to biostratigraphy, sequence stratigraphy, environments of deposition, and diagenesis. J. Sediment. Res. 68, 1212–1222.

Head, J.W., 1969. An Integrated Model of Carbonate Depositional Basin Evolution: Late Cayugan (Upper Silurian) and Helderbergian (Lower Devonian) of the Central Appalachians, unpubl. Ph.D. dissertation. Brown University, Providence, RI, 390 pp.

Helfrich, C.T., 1978. A conodont fauna from the Keyser Limestone of Virginia and West Virginia. J. Paleontol. 52, 1133–1142.

Hladikova, J., Hladil, J., Kribek, B., 1997. Carbon and oxygen isotope record across Pridoli to Givetian stage boundaries in the Barrandian basin (Czech Republic). Palaeogeogr. Palaeoclimatol. Palaeoecol. 132, 2225–2241.

Hladil, J., 1991. Evaluation of the sedimentary record in the Silurian–Devonian boundary stratotype at Klonk (Barrandian area, Czechoslovakia). Newsl. Stratigr. 25 (2), 115–125.

Hoffman, P.F., Kaufman, A.J., Halverson, G.P., Schrag, D.P., 1998. A Neoproterozoic snowball earth. Science 281, 1342–1346.

Jeppsson, L., 1988. Conodont biostratigraphy of the Silurian–Devonian boundary at Klonk, Czechoslovakia. Geol. Palaeontol. 22, 21–31.

Jeppsson, L., 1989. Latest Silurian conodonts from Klonk, Czechoslovakia. Geol. Palaeontol. 23, 21–37.

Joachimski, M.M., Buggisch, W., 1993. Anoxic events in the late Frasnian: causes of the Frasnian–Famennian faunal crisis? Geology 21, 675–678.

Johnson, J.G., Murphy, M.A., 1984. Time–rock model for Siluro–Devonian continental shelf, western United States. Geol. Soc. Am. Bull. 95, 1349–1359.

Johnson, J.G., Klapper, G., Sandberg, C.A., 1985. Devonian eustatic fluctuations in Euramerica. Geol. Soc. Am. Bull. 96, 567–587.

Johnson, K.S., 1993. Hunton Group Core Workshop and Field Trip. Okla. Geol. Surv. Spec. Publ. 93-4, 212 pp.

Johnson, M.E., 1996. Stable cratonic sequences and a standard for Silurian eustasy. In: Witzke, B.J., et al. (Eds.), Paleozoic Sequence Stratigraphy: Views from the North American Craton. Spec. Paper Geol. Soc. Am. 306, 203–311.

Kaljo, D., Kiipli, T., Martma, T., 1997. Carbon isotope event markers through the Wenlock–Pridoli sequence at Ohesaare (Estonia) and Priekule (Latvia). Palaeogeogr. Palaeoclimatol. Palaeoecol. 132, 211–223.

Kaufman, A.J., Hayes, J.M., Knoll, A.H., Germs, G.J.B., 1991. Isotopic compositions of carbonates and organic carbon from Upper Proterozoic successions in Namibia: stratigraphic variation and the effects of diagenesis and metamorphism. Precambrian Res. 49, 301–327.

Klapper, G., Murphy, M.A., 1975. Silurian–Lower Devonian Conodont Sequence in the Roberts Mountains Formation of Central Nevada. University of California Publications in Geological Sciences 111, 62 pp.

Kump, L.R., Arthur, M.A., Patzkowsky, M.E., Gibbs, M.T., Pinkus, D.S., Sheehan, P.M., 1999. A weathering hypothesis for glaciation at high atmospheric pCO_2 during the Late Ordovician. Palaeogeogr. Palaeoclimatol. Palaeoecol. 152, 173–187.

Kump, L.R., Arthur, M.A., 1999. Interpreting carbon-isotope excursions: carbonates and organic matter. Chem. Geol. 161, 181–198.

Kriz, J., 1991. The Silurian of the Prague Basin (Bohemia): Tectonic, eustatic, and volcanic controls on facies and faunal development. In: Special Papers in Palaeontology 44, 179–204.

Magaritz, M., 1983. Carbon and oxygen isotope composition of recent and ancient coated grains. In: Peryt, T.M. (Ed.), Coated Grains. Springer, Berlin, pp. 27–37.

Matti, J.C., McKee, E.H., 1977. Silurian and Lower Devonian paleogeography of the outer continental shelf of the Cordilleran Miogeocline, central Nevada. In: Stewart, J.H., Stevens, C.H., Fritsche, A.E. (Eds.), Paleozoic Paleogeography of the Western United States – Pacific Section. SEPM, Los Angelos, CA, pp. 181–215.

Mii, H., Grossman, E.L., Yancey, T.E., 1999. Carboniferous isotope stratigraphies of North America: implications for Carboniferous paleoceanography and Mississippian glaciation. Geol. Soc. Am. Bull. 111, 960–973.

Poole, F.G., Sandberg, C.A., Boucot, A.J., 1977. Silurian and Devonian paleogeography of the western United States. In: Stewart, J.H., Stevens, C.H., Fritsche, A.E. (Eds.), Paleozoic Paleogeography of the Western United States – Pacific Section. SEPM, Los Angelos, CA, pp. 39–65.

Porebska, E., Sawlowicz, Z., 1997. Palaeoceanographic linkage of geochemical and graptolite events across the Silurian–Devonian boundary in Bardzkie Mountains (Southwest Poland). Palaeogeogr. Palaeoceanogr. Palaeoclimatol. 132, 343–354.

Ripperdan, R.L., Magaritz, M., Nicoll, R.S., Shergold, J.H., 1992. Simultaneous changes in carbon isotopes, sea-level and conodont biozones within the Cambrian–Ordovician boundary interval at Black Mountain, Australia. Geology 20, 1039–1042.

Saltzman, M.R., Runnegar, B., Lohmann, K.C., 1998. Carbon-isotope stratigraphy of the Pterocephaliid Biomere in the eastern Great Basin: record of a global oceanographic event during the Late Cambrian. Geol. Soc. Am. Bull. 110, 285–297.

Saltzman, M.R., Brasier, M.D., Ripperdan, R.L., Ergaliev, G.K., Lohmann, K.C., Robison, R.A., Chang, W.T., Peng, S., Runnegar, B., 2000a. A global carbon isotope excursion during the Late Cambrian: relation to trilobite extinctions, organic-matter burial and sea level. Palaeogeogr. Palaeoceanogr. Palaeoclimatol. 162, 211–223.

Saltzman, M.R., Gonzalez, L.A., Lohmann, K.C., 2000b. Earliest Carboniferous cooling step triggered by the Antler Orogeny? Geology 28, 347–350.

Saltzman, M.R., 2001. Silurian $\delta^{13}C$ stratigraphy: a view from North America. Geology 29, 671–674.

Saltzman, M.R., 2002. Carbon and oxygen isotope stratigraphy of the Lower Mississippian (Kinderhookian–early Osagean), western United States: implications for seawater chemistry and glaciation. Geol. Soc. Am. Bull. 114, 96–108.

Sartain, R.R., 1981. Stratigraphy and conodont paleontology of Late Silurian–Early Devonian strata of western Virginia. unpubl. M.Sc. Thesis, Virginia Polytech. Inst., Blacksburg, VA, 151 pp.

Saylor, B.Z., Kaufman, A.J., Grotzinger, J.P., Urban, F.A., 1998. Composite reference section for terminal Proterozoic strata of southern Namibia. J. Sediment. Res. 68, 1223–1235.

Schonlaub, H.P., 1986. Significant geological events in the Paleozoic record of the southern Alps (Austrian part). In: Walliser, O.H. (Ed.), Global Bio-Events. Lecture Notes in Earth Sciences 8, Springer, Berlin, pp. 163–167.

Schonlaub, H.P., Kreutzer, L.H., Joachimski, M.M., Buggisch, W., 1994. Paleozoic boundary sections of the Carnic Alps (Southern Austria). Erlanger Geol. Abh. 122, 77–103.

Scotese, C.R., McKerrow, W.S., 1990. Revised world maps and introduction. Geol. Soc. London, Mem. 12, 1–21.

Shaver, R.H., 1996. Silurian sequence stratigraphy in the the North American Craton, Great Lakes area. In: Witzke, B.J., Ludvigson, G.A., Day, J. (Eds.), Paleozoic Sequence Stratigraphy: Views from the North American Craton, Spec. Paper. Geol. Soc. Am. 306, 193–202.

Sheehan, P.M., Boucot, A.J, 1991. Silurian paleogeography of the Western United States. In: Cooper, J.D., Stevens, C.H. (Eds.), Paleozoic Paleogeography of the Western United States II – Pacific Section. Society of Economic Paleontologists and Mineralogists, pp. 51–82.

Sloss, L.L., 1963. Sequences in the cratonic interior of North America. Geol. Soc. Am. Bull. 74, 93–114.

Trojan, W.R., 1979. Devonian stratigraphy and depositional environments of the northern Antelope Range, Eureka County, Nevada. Unpubl. M.Sc. Thesis, Oregon State University, Corvallis, OR, 134 pp.

Wang, K., Geldsetzer, H.H.J., Goodfellow, W.D., Krouse, H.R., 1996. Carbon and sulfur isotope anomalies across the Frasnian–Famennian extinction boundary, Alberta, Canada. Geology 24, 187–191.

Wenzel, B., Joachimski, M.M., 1996. Carbon and oxygen isotopic composition of Silurian brachiopods (Gotland/Sweden): palaeoceanographic implications. Palaeogeogr. Palaeoclimatol. Palaeoecol. 122, 143–166.

Wigforss-Lange, J., 1999. Carbon isotope ^{13}C enrichment in Upper Silurian (Whitcliffian) marine calcareous rocks in Scania, Sweden. GFF (Geological Society of Sweden) 121, 273–279.

Witzke, B.J., 1990. Palaeoclimatic constraints for Palaeozoic palaeolatitudes of Laurentia and Euramerica. In: McKerrow, W.S., Scotese, C.R. (Eds.), Palaeozoic Palaeogeography and Biogeography. Geological Society London Memoir 12, 57–73.

Witzke, B.J., Bunker, B.J., 1996. Relative sea-level changes during Middle Ordovician through Mississippian deposition in the Iowa area, North American Craton. In: Witzke, B.J., Ludvigson, G.A., Day, J. (Eds.), Paleozoic Sequence Stratigraphy: Views from the North American Craton. Spec. Paper Geol. Soc. Am. 306, 307–330.